J Therm Anal Calorim (2012) 109:727–734
DOI 10.1007/s10973-012-2454-8

Synthesis, thermal behavior, and other properties of Y(III) and La(III) complexes with 4,4′-bipyridine and trichloro- or dibromoacetates

A. Czylkowska · M. Markiewicz

Bretsznajder Special Chapter

Abstract New Y(III) and La(III) complexes with 4-bpy (4,4′-bipyridine) and trichloro- or dibromoacetates with the formulae: $Y(4\text{-bpy})_2(CCl_3COO)_3{\cdot}H_2O$ **I**, $La(4\text{-bpy})_{1.5}(CCl_3COO)_3{\cdot}2H_2O$ **II**, $Y(4\text{-bpy})_{1.5}(CHBr_2COO)_3{\cdot}3H_2O$ **III**, and $La(4\text{-bpy})(CHBr_2COO)_3{\cdot}H_2O$ **IV** were prepared and characterized by chemical, elemental analysis, and IR spectroscopy. Conductivity studies (in methanol, dimethyloformamide, and dimethylsulfoxide) were also described. They are small, crystalline substances. The way of metal–ligand coordination was discussed. The thermal properties of complexes in the solid state were studied by TG-DTG techniques under dynamic flowing air atmosphere. TG-FTIR system was used to analyze principal volatile thermal decomposition and fragmentation products evolved during pyrolysis in dynamic flowing argon atmosphere for La(III) compounds.

Keywords Y(III) and La(III) complexes · 4,4′-Bipyridine · Trichloroacetates · Dibromoacetates · TG-DTG · TG-FTIR · IR spectra

Introduction

The lanthanide compounds including N- and O-donors, as 4-bpy and carboxylate groups are very interesting because of their structural diversity and also possibility to use as new solid microporous materials. These coordination compounds have high microporosity comparing to conventional porous materials such as zeolites or activated carbon. They have various possible applications in ion exchange, gas storage (CH_4, H_2, N_2, O_2, and CO_2), gas separation, heretogeneous catalysis, etc. [1]. These types of compounds are still actual in researches. 4,4′-Bipyridine is used as a potential ligand since two nitrogen donor atoms. This N-donor may create polymeric species [2–6]. Up to now, there are not many papers describing lanthanides complexes with bipyridine isomers and halogenoacetates [7–11].

This work is a continuation of our studies, and presents the synthesis, some physico-chemical properties, and thermal investigations of new complexes of Y(III) and La(III) with title ligands.

Earlier, we had obtained the compounds with N-donor (4-bpy) and dichloroacetates of Y(III) and La(III) with general formulae: $Y(4\text{-bpy})(CHCl_2COO)_3{\cdot}H_2O$ and $[La(4,4'\text{-bipyridine})(CCl_2HCOO)_3(H_2O)]_n$ were described in [6, 12]. They were characterized by elemental and thermal analysis, IR, and conductivity studies. The crystal and molecular structure of lanthanum(III) complex [6] were determinated.

Experimental

Materials, synthesis, and analysis

4,4′-Bipyridine, CCl_3COOH, $CHBr_2COOH$, Y_2O_3, La_2O_3, dimethylsulfoxide (DMSO), dimethylformamide (DMF), and methanol (MeOH) (anhydrous) p.a. were obtained from Aldrich and Lab-Scan. Water solutions of metal(III) trichloroacetates or metal(III) dibromoacetates were prepared by adding 2 mol L^{-1} trichloro- or dibromoacetic acid to freshly precipitated hydroxides in ca. stoichiometric quantities (in temperature $\leq$291 K, because lanthanide

A. Czylkowska (✉) · M. Markiewicz
Institute of General and Ecological Chemistry, Technical University of Lodz, Lodz, Poland
e-mail: agnieszka.czylkowska@p.lodz.pl

trichloro- and dibromoacetates in solution are relatively unstable; in the presence of 4-bpy, their stability arise). The contents of metal(III) ions in obtained solutions were complexometrically determined. The synthesis of complexes was analogous, as described in [13].

The carbon, hydrogen, and nitrogen contents in the prepared complexes were determined by a Carbo-Erba analyzer using V_2O_5 as an oxidizing agent. Obtained compounds were mineralized and metals(III) in describe complexes were determined by EDTA titration.

Methods and instruments

IR spectra were recorded using a NICOLETT 6700 Spectrometer (4000–400 cm^{-1} with accuracy of recording 1 cm^{-1}) using KBr pellets. Molar conductance was measured on a conductivity meter of the OK-102/1 type equipped with an OK-902 electrode at 298 ± 0.5 K, using 1×10^{-3} mol L^{-1} solutions of complexes in methanol, dimethylformamide, and dimethylsulfoxide. The thermal properties of complexes in air were studied by TG-DTG techniques in the range of temperature 298–1273 K at a heating rate of 10 K min^{-1}; TG and DTG curves were recorded on Netzsch TG 209 apparatus in flowing dynamic air atmosphere $v = 20$ mL min^{-1} using ceramic crucibles. From TG and DTG curves, some of the solid intermediate decomposition products were determined and were confirmed by the IR spectra of sinters. In sinters (prepared during heating of complexes up to temperatures defined from TG or DTG curves), the vibration modes of 4-bpy and halogenoacetates were analyzed as well as the presence of anions Cl^- or Br^- were also stated. The TG-FTIR coupled measurements have been carried out only for complexes **II** and **IV** using the Netzsch TG 209 apparatus coupled with Bruker FTIR spectrophotometer, in the range of temperature 293–973 K at a heating rate 10 K min^{-1} in flowing argon atmosphere $v = 20$ mL min^{-1} in ceramic crucibles. The X-ray powder diffraction patterns of synthesized complexes and final solid decomposition products in air were recorded on D-5000 diffractometer using Ni-filtered CuK_α radiation. The measurements were carried out in the range of 2θ angles 2–80°. Obtained results were analyzed using the Powder Diffraction File [14].

Results and discussion

Table 1 presents results of the elemental and chemical analysis of investigated compounds. They are stable in air in solid state and the monocrystals of them have not been obtained yet. The analysis of the power diffraction patterns of these compounds reveals that they are small crystalline products. The molar conductivity values for complexes in MeOH, DMF, and DMSO are given in Table 1. La(4-bpy)$(CHBr_2COO)_3 \cdot H_2O$ in DMSO, complexes **I–IV** in MeOH, and **II–IV** in DMF display behaviors intermediate between those of non-electrolytes and 1:1 electrolytes. The compound **III** in DMSO is electrolyte type 1: 1. Y(4-bpy)$_2(CCl_3COO)_3 \cdot H_2O$ in DMF, Y(4-bpy)$_2(CCl_3COO)_3 \cdot H_2O$ and La(4-bpy)$_{1.5}(CCl_3COO)_3 \cdot 2H_2O$ in DMSO fall within the generally acceptable range for non-electrolytes. Very low molar conductance values indicate the non-electrolytic nature of them [15].

IR spectra

IR spectra of all the obtained complexes exhibit several absorption bands characteristic for 4-bpy and carboxylate groups.

The fundamental vibration modes of 4-bpy for complexes are reported in Table 2. During coordination with lanthanide ions, the IR spectrum of free 4,4′-bipyridine changes. The most characteristic ring vibration modes ν(CC), ν(CN), $\nu(CC_{ir})$-A_1 symmetry, and ν(CC), ν(CC)-B_1 symmetry are at 1588 and 1530 cm^{-1} in the free ligand [16]. In the IR spectra of complexes, they appear at 1600–1608 and 1530–1539 cm^{-1}, respectively. The ring deformation modes are noticed between 1000–1003 cm^{-1} and are shifted to higher frequencies in comparison with free 4-bpy (988 cm^{-1}). These bathochromic shifts of principal absorption bands suggest that 4-bpy is coordinated to Y(III) and La(III) ions [16].

Table 1 Analytical data and molar conductivity in MeOH, DMF, and DMSO for investigated complexes

Compound		Analysis: found (calculated)/%				Λ_M (Ω^{-1} cm^2 mol^{-1}); $c = 1 \times 10^{-3}$ mol L^{-1}		
		Ln	C	N	H	MeOH	DMF	DMSO
I	Y(4-bpy)$_2(CCl_3COO)_3 \cdot H_2O$	9.76 (9.81)	34.52 (34.45)	6.21 (6.18)	1.98 (2.00)	55.5	5.0	2.6
II	La(4-bpy)$_{1.5}(CCl_3COO)_3 \cdot 2H_2O$	15.62 (15.50)	28.18 (28.14)	4.72 (4.69)	1.78 (1.80)	58.0	41.1	2.9
III	Y(4-bpy)$_{1.5}(CHBr_2COO)_3 \cdot 3H_2O$	8.66 (8.65)	24.49 (24.54)	4.07 (4.09)	2.05 (2.06)	67.0	51.0	52.3
IV	La(4-bpy)$(CHBr_2COO)_3 \cdot H_2O$	14.48 (14.41)	19.91 (19.94)	2.89 (2.91)	1.37 (1.36)	51.0	36.0	41.0

Table 2 IR bands for free 4- and 4-bpy in the obtained complexes

4-bpy [16]	Complexes				Assigments
	I	**II**	**III**	**IV**	
1588	1600	1601	1601	1608	υ(CC), υ(CN), $\upsilon(CC_{ir})$, A_1
		1560			
1530	1539	1533	1534	1530	υ(CC), υ(CN) B_1
1488	1489	1488	1489	1489	υ(CC), υ(CN)
		1458			
1403	1412	1410	1411	1415	υ(CC), υ(CN)
1328	–	–	1330	1330	υ(CC), υ(CN)
1205	1218	1218	1220	1220	β(CH)
1092	1100	1100	1100	–	β(CH)
1072	1068	1067	1065	1066	β(CH)
1037	1045	1042	1043	1045	"ring breathing"
988	1001	1002	1003	1000	"ring breathing"
962	950[a]	960[a]	–	960	γ(CH)
850	–	–	850	850	γ(CH)
810	806	802	804	808	γ(CH)
745	[a]	[a]	745	750	γ(CH)
733	737	731	718	714	γ(CH)
672	[a]	[a]	688	687	γ(CH)
608	620	615	623	621	β(CH)
572	572	572	587	595	β(CH)
500	500	500	500	500	β(CH)

ir inter ring bands; A_1-symmetry A_1, B_1-symmetry B_1

[a] Overlap by CCl_3COO^- absorption

Table 3 IR bands for CCl_3COONa and COO^- groups in the obtained complexes

CCl_3COONa [19]	Complexes		Assigments
	I	**II**	
1677	1674	1677	ν_{as}(COO)
	1636	1656	
1353	1382	1366	ν_s(COO)
	1346		
940	[a]	[a]	ν(CC)
849	–	–	$\nu_{as}(CCl_3)$
833	838	837	$\nu_{as}(CCl_3)$
746	768[a]	756[a]	$\nu_s(CCl_3)$
685	684[a]	684[a]	$\nu_s(CCl_3)$
324	292	311	$\Delta\nu = \nu_{as}-\nu_s$
	290	290	

[a] Overlap by 4-bpy absorption

Table 4 IR bands for $CHBr_2COONa$ and COO^- groups in the obtained complexes

$CHBr_2COONa$ [19]	Complexes		Assigments
	III	**IV**	
3015	3027	3020	ν(CH)
1616	1650	1663	ν_{as}(COO)
1378	1389	1386	ν_s(COO)
1191	1186	1192	ν(CH)
1148	1150	1150	δ(CCOO)
931	920	930	ν(CC)
698	700	700	$\nu_s(CBr_2)$
238	261	277	$\Delta\nu = \nu_{as}-\nu_s$

In the IR spectra, there are also bands of vibrations of asymmetric ν_{as}(COO) and symmetric ν_s(COO) modes for carboxylate groups (Tables 3, 4). For complexes **I** and **II**, they are in the range 1636–1677 and 1346–1382 cm^{-1}, respectively. In both case, the ν_{as}(COO) and for compound **I** also ν_s(COO) are split into doublet. The carboxylate groups in complexes **I** and **II** act as bidentate-chelating, non-completely equivalent [17] (more or less symmetrical [18]) ligands. For complexes **I** and **II**, vibrations $\nu_{as}(CCl_3)$ are shifted to higher wave numbers according to CCl_3COONa. In the case of compounds $Y(4\text{-bpy})_{1.5}(CHBr_2COO)_3{\cdot}3H_2O$ **III** and $La(4\text{-bpy})(CHBr_2COO)_3{\cdot}H_2O$ **IV**, the

bands of vibrations of ν_{as}(COO) and ν_s(COO) are between 1650–1663 and 1386–1389 cm^{-1}, respectively. On the grounds of spectroscopic criteria [19–22], it can be stated that in complexes **III** and **IV** carboxylate groups are bonded as monodentate donors (the values of $\Delta\nu = \nu_{as} - \nu_s$ of these complexes are higher than for sodium salt). The vibrations of ν(CH) appear in sodium salt at 3015 and 1191 cm^{-1}, in complexes are at 3027 cm^{-1} for **III**, 3020 cm^{-1} for **IV**, and at 1186 cm^{-1} in spectra of **III**, 1192 cm^{-1} in the case of **IV**. The stretching modes $\nu_s(CBr_2)$ in $Y(4\text{-bpy})_{1.5}(CHBr_2COO)_3{\cdot}3H_2O$ and $La(4\text{-bpy})(CHBr_2COO)_3{\cdot}H_2O$ are observed at 700 cm^{-1}. The vibrations δ(CCOO) at 1148 cm^{-1} in $CHBr_2COONa$ spectra, in compounds **III** and **IV** appear at 1150 cm^{-1}.

All the complexes exhibit intensive and broad band in the water stretching region (ca 3560–3350 cm^{-1}) and only shoulder in the water bending region (ca 1730–1690 cm^{-1}).

Thermogravimetric data in air

The thermal decompositions of described complexes have been studied in air by TG-DTG method. Pyrolysis of analyzing complexes in air is a multistage, overlapping process and complicated to interpret. Several steps of thermolysis and the solid products were determined from TG and DTG curves. Some intermediate species were verified by investigation of the sinters obtained during heating of the samples of complexes up to temperature defines from the thermal curves. The intensity of DTG peaks is different. When temperature rises, the peaks on DTG profiles are weaker. All compounds lose water molecules in one step. When temperature rises, decomposition of halogenoacetates begins and intermediate products are formed. Figures 1, 2, 3, and 4 show thermal profiles of investigated complexes. Table 5 presents thermal decomposition results of Y(III) and La(III) compounds in air and only La(III) complexes in argon atmosphere.

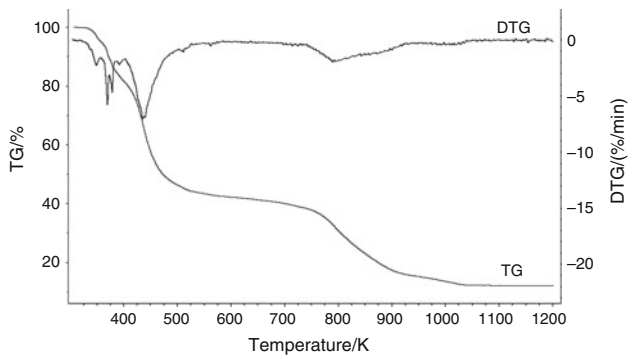

Fig. 1 TG and DTG curves of thermal decomposition of $Y(4\text{-bpy})_2(CCl_3COO)_3{\cdot}H_2O$ recorded in air atmosphere; mass sample 5.99 mg

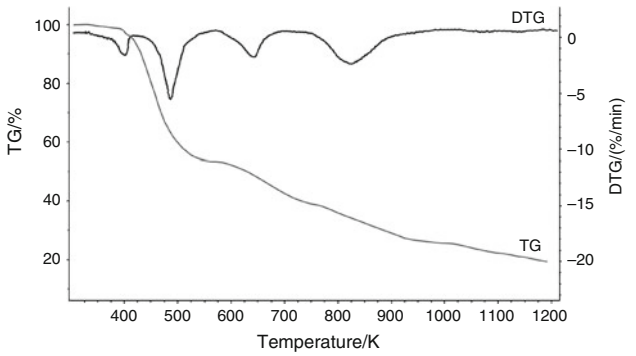

Fig. 2 TG and DTG curves of thermal decomposition of $La(4\text{-bpy})_{1.5}(CCl_3COO)_3{\cdot}2H_2O$ recorded in air atmosphere; mass sample 7.41 mg

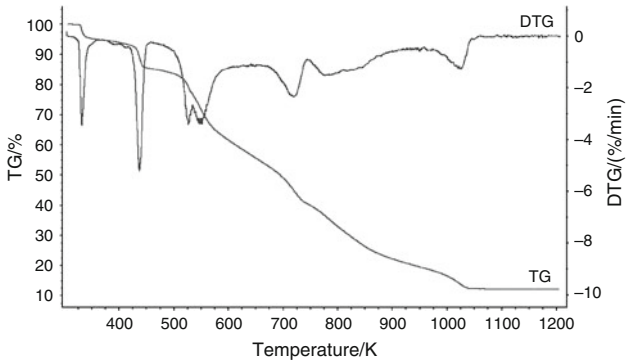

Fig. 3 TG and DTG curves of thermal decomposition of $Y(4\text{-bpy})_{1.5}(CHBr_2COO)_3{\cdot}3H_2O$ recorded in air atmosphere; mass sample 8.03 mg

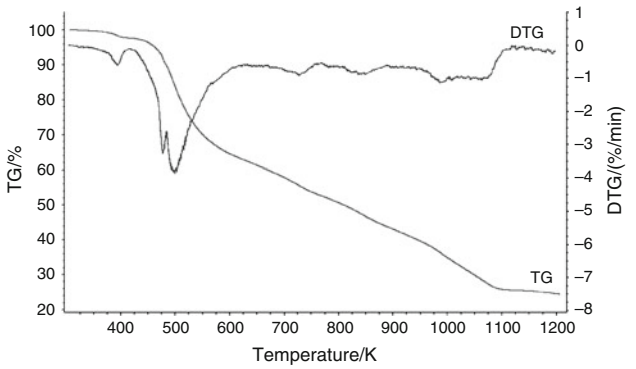

Fig. 4 TG and DTG curves of thermal decomposition of $La(4\text{-bpy})(CHBr_2COO)_3{\cdot}H_2O$ recorded in air atmosphere; mass sample 9.67 mg

Thermal decomposition of complexes **I** and **II** in air begins at 333 K. It is associated with the release of all water molecules. Mass losses calculated for dehydration processes are 1.99 % for **I** and 4.02 % for **II**, when these determined from the thermogravimetric curves are 2.2 % and 4.0 %, respectively. In the second step, the anhydrous compound

Table 5 Thermal decomposition data (A) for Y(III) and La(III) complexes in air; (B) only for La(III) compounds in argon atmosphere

No.	Compound	Range of decomposition /K	DTG peaks / K	Mass loss / %		Products
				Found	Calc	
A) thermal decomposition data in air atmosphere						
I	$Y(4\text{-bpy})_2(CCl_3COO)_3{\cdot}H_2O$	333–353	343	2.2	1.99	$Y(4\text{-bpy})_2(CCl_3COO)_3$
		353–375	368	7.2	7.00	$Y(4\text{-bpy})_2(CCl_3COO)_{2.5}Cl_{0.5}$
		375–383, 383–403, 403-723, 723-923	378, 393, 438, 793	74.4	75.53	YOCl
		923-1038		3.7	3.02	Y_2O_3
II	$La(4\text{-bpy})_{1.5}(CCl_3COO)_3{\cdot}2H_2O$	333–413	400	4.0	4.02	$La(4\text{-bpy})_{1.5}(CCl_3COO)_3$
		413–571	483	42.5	42.56	$La(4\text{-bpy})_{1.5}Cl_3$
		571–763, 763-933	643, 825	26.5	26.10	$LaCl_3$
		>933				very slowly converted to La_2O_3
III	$Y(4\text{-bpy})_{1.5}(CHBr_2COO)_3{\cdot}3H_2O$	328–373	333	5.0	5.26	$Y(4\text{-bpy})_{1.5}(CHBr_2COO)_3$
		373–453	438	9.6	9.99	$Y(4\text{-bpy})_{1.5}(CHBr_2COO)_{2.25}Br_{0.75}$
		453–533, 533-643, 643-743, 743-975	523, 548, 718, 775–840 br	67.6	66.77	YOBr
		975–1043	1023	6.5	6.99	Y_2O_3
IV	$La(4\text{-bpy})(CHBr_2COO)_3{\cdot}H_2O$	373–418	398	1.7	1.87	$La(4\text{-bpy})(CHBr_2COO)_3$
		418–483	475	8.6	7.13	$La(4\text{-bpy})(CHBr_2COO)_{2.25}Br_{0.75}$
		483-623, 623-763, 763-958, 958–1113	498, 728, 840, 983–1060 br	64.8	66.60	LaOBr
B) thermal decomposition data in argon atmosphere						
II	$La(4\text{-bpy})_{1.5}(CCl_3COO)_3{\cdot}2H_2O$	333–453	423	4.7	4.02	$La(4\text{-bpy})_{1.5}(CCl_3COO)_3$
		453–553	507	38.0	38.94	$La(4\text{-bpy})_{1.5}(CCl_3COO)_{0.25}Cl_{2.75}$
		553–953		11.0		mixture of organic and inorganic residue
IV	$La(4\text{-bpy})(CHBr_2COO)_3{\cdot}H_2O$	353–433	403	2.0	1.87	$La(4\text{-bpy})(CHBr_2COO)_3$
		433–633, 633-933	493sh 513, 703	53.5		mixture of organic and inorganic residue

br broad, *sh* shoulder

$Y(4\text{-bpy})_2(CCl_3COO)_3$ decomposes probably (in temperature range 353-375 K) to $Y(4\text{-bpy})_2(CCl_3COO)_{2.5}Cl_{0.5}$ (mass loss: found. 7.2 %; calc. 7.00 %). This step is clearly presented on DTG curve (strong peak at 368 K). We have also similar observations in the case of complex $Y(4\text{-bpy})(CCl_2HCOO)_3H_2O$ described in [12]. Elevation of temperature induces that several peaks on DTG curve and mass losses are observed. It is connected with further decomposition of organic ligands and produces other intermediate decomposition products (which are not examined). At temperature 923 K, stoichiometry quantity equivalent for YOCl is indicated from TG curve. It connects with peak on DTG curve at 793 K. At 1038 K, the final pure product Y_2O_3 is obtained (found 12.5 %, calculated 12.46 %). In the case of anhydrous complex **II**, the DTG curve exhibits at 483 K a sharp peak indicating the maximum mass loss rate (42.5 %). It is connected with total decomposition of chloroacetates. When temperature increases, on DTG curve, peaks appear at 643 and 825 K. The TG and DTG curves suggest that at 933 K probably $LaCl_3$ exists (found. 27.0 %; calc. 27.32 %). When temperature rises, it very slowly undergoes further destruction to La_2O_3.

For both complexes $Y(4\text{-bpy})_{1.5}(CHBr_2COO)_3{\cdot}3H_2O$ **III** and $La(4\text{-bpy})(CHBr_2COO)_3{\cdot}H_2O$ **IV**, the first mass loss observed on TG curves corresponds to evaluation of all water molecules in temperature interval 328–373 and

373–418 K, respectively. Probably in temperature range 373–453 K for **III** the partial destruction of dibromoacetate groups takes place and intermediate species Y(4-bpy)$_{1.5}$(CHBr$_2$COO)$_{2.25}$·Br$_{0.75}$ is formed (mass loss found. 9.6 %; calc. 9.99 %). It is connected with very strong peak on DTG curve at 438 K. Next, further step-wise decomposition of organic ligands occurs (thermogravimetric curves show the presence of several overlap processes). In temperature range 533-975 K, mass loss observed on the thermal curve is associated with total destruction and combustion of organic ligands, YOBr is formed. Above 975 K, YOBr transforms to Y_2O_3. Horizontal mass level for Y_2O_3 begins at 1043 K (found 11.3 %, calc. 10.99 %). Anhydrous compound **IV** starts to decompose at 418 K. This pyrolysis is very similar to the thermal decomposition data of studied complexes. The solid product of thermolysis obtained at 1113 K is LaOBr (found. 24.9 %; calc. 24.40 %).

TG-FTIR study for La(III) complexes in argon

The combined TG-FTIR techniques was employed to study thermal decomposition and the gas generated in flowing argon atmosphere only for La(III) complexes. TG and DTG profiles of complexes **II** and **IV** are shown in Figs. 5 and 6. Thermal decomposition data are collected in Table 5. Dehydration of compound **II** takes place in the range 333–453 K, while elimination of water for complex **IV** occurs between the range 353–433 K. The mass loss from this process is expected to be 4.02 % for **II** and 1.87 % in the case of **IV**; recorded 4.7 % and 2.0 %, respectively. Anhydrous complexes start to decompose at 453 K for **II** and 433 K for **IV** with several overlapping stages. The sharp DTG peak at 507 K for **II** and peak at 513 K with a shoulder at 493 K for **IV**; in both cases they correspond to a rapid loss in mass. This decrease in mass ascribed to stepwise decomposition of halogenoacetate ligands (*vide* FTIR spectra). Next, degradation of organic ligands takes place. The pyrolysis for **II** is finished at about 953 K, residual 46.3 %. In the case of **IV**, residual is at 933 K and has a value 44.5 %. It is probably due to the mixture of inorganic species and solid organic fragments. The compositions of these products were not investigated.

The elevation of the gaseous products during decomposition of the La(4-bpy)$_{1.5}$(CCl$_3$COO)$_3$·2H$_2$O and La(4-bpy)(CHBr$_2$COO)$_3$·H$_2$O are shown in Figs. 7 and 8. The TG-FTIR spectra for compounds **II** and **IV** are very similar, but the peaks can be attributed to the volatile species of halogen-containing groups. The selected vibration modes are only indicated on FTIR spectra in different thermal intervals. The assignment of peaks in the FTIR spectra was attributed by comparison with literature data [1, 20, 23]. The recorded spectra confirms that the first step of thermal decomposition of compound **II** is dehydration process (absorption peaks between 3750–3550 cm^{-1}).

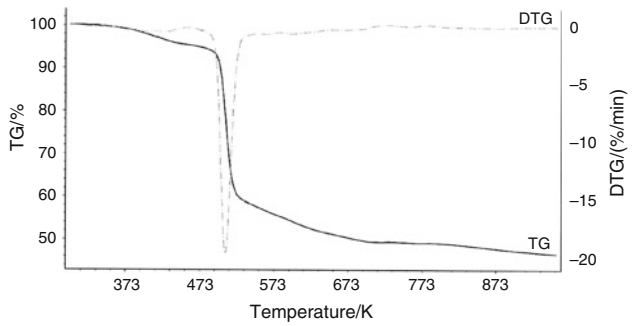

Fig. 5 TG and DTG curves of thermal decomposition of La(4-bpy)$_{1.5}$(CCl$_3$COO)$_3$·2H$_2$O recorded in argon atmosphere; mass sample 14.65 mg

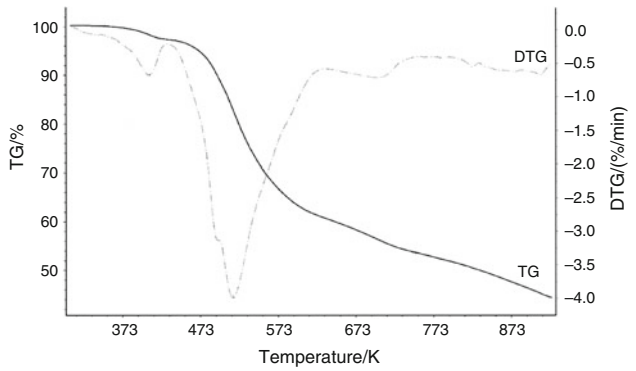

Fig. 6 TG and DTG curves of thermal decomposition of La(4-bpy)(CHBr$_2$COO)$_3$·H$_2$O recorded in argon atmosphere; mass sample 9.35 mg

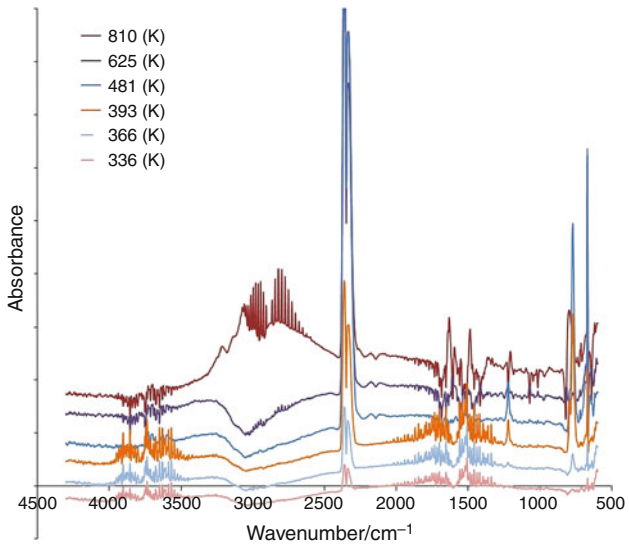

Fig. 7 Typical FTIR spectra in argon of gaseous species produced during decomposition of La(4-bpy)$_{1.5}$(CCl$_3$COO)$_3$·2H$_2$O in different temperatures

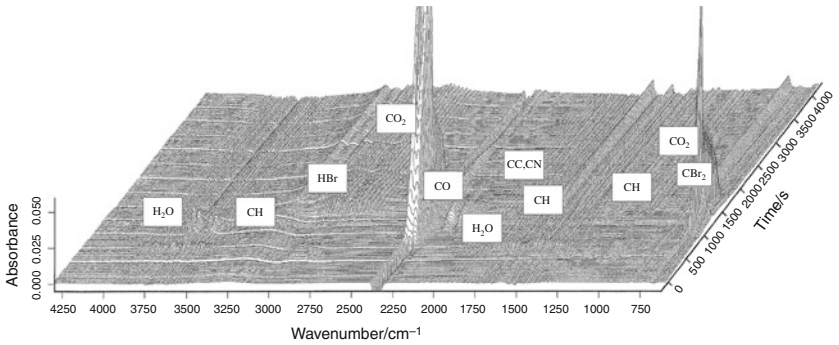

Fig. 8 Stacked plot of FTIR spectra of the evolved gases for La(4-bpy)$(CHBr_2COO)_3{\cdot}H_2O$ complex in argon

Decomposition of the desolvated form of the compound is connected with emission of CO_2 molecules. It gives the characteristic double bands at 2360–2280 and 720–640 cm^{-1}, which ascribes to the valence and deformation vibrations, respectively. The maximum elevation for compound **II** is observed at 508 K, which is strictly the same temperature that the sharp DTG peaks (507 K). In the case of La(4-bpy)
$(CHBr_2COO)_3{\cdot}H_2O$, the maximum rate of forming CO_2 is at ca 494 K; DTG peak at 513 K with a shoulder at 493 K. When temperature rises, the emission of CO_2 decreases. It may be imply the final stage of decomposition of carboxylate groups. The double band locates at 2250–2150 cm^{-1} can be attributed to carbon monoxide. The absorption bands of vibrations of CH groups evolving from hydrocarbons lie between 3050–2680 cm^{-1} for **II** and 3035–2800 cm^{-1} for compound **IV**. The vibration modes of β(CH) in plane for **II** and **IV** are observed at 1265 and 1300 cm^{-1}, respectively. However, γ(CH) out of plane are recorded in the range 800–750 cm^{-1} in both cases. The fragments of 4-substituted pyridine (ν(CC), ν(CN)) for investigated complexes are detected between 1600–1580 cm^{-1}. In addition, during thermal decomposition of these complexes, the evaluations of volatile species containing halogen are produced. The FTIR spectra of the complex **II** shows absorption bands at ca 840 cm^{-1} and 745, 680 cm^{-1}, which are assigned to the $\nu_{as}(CCl_3)$ and $\nu_s(CCl_3)$, respectively. On the other hand, for compound **IV** only $\nu_s(CBr_2)$ at 695 cm^{-1} occurs. The absorption modes of HBr were found at ca 2355 cm^{-1}.

Conclusions

Here, we describe new complexes with formulae: Y(4-bpy)$_2(CCl_3COO)_3{\cdot}H_2O$, La(4-bpy)$_{1.5}(CCl_3COO)_3{\cdot}2H_2O$, Y(4-bpy)$_{1.5}(CHBr_2COO)_3{\cdot}3H_2O$, and La(4-bpy)$(CHBr_2COO)_3{\cdot}H_2O$. It courses, that La(4-bpy)$(CHBr_2COO)_3{\cdot}H_2O$ has the same stoichiometric formula as La(4-bpy)$(CHCl_2COO)_3{\cdot}H_2O$ [6]. They are small, crystalline substances. On the base of IR spectra of these compounds, it may be stated that 4,4′-bipyridine coordinates to metal(III) ions [16]; carboxylate groups in complexes **I** and **II** act as bidentate-chelating, non-completely equivalent [17] (more or less symmetrical [18]) ligands; in case of compounds **III** and **IV** carboxylate groups are linked with metal(III) as monodentate donors [19–22]. The thermal decomposition of the described complexes in flowing dynamic air atmosphere is a multistage and overlapping process. In all cases, dehydration is the first step of pyrolysis. Next, partial and total decomposition of organic ligands takes place. The final solid products of thermolysis are: Y_2O_3 for **I** and **III**. In the case of lanthanum(III) complexes were not observed horizontal mass level.

Comparing complex Y(4-bpy)$(CHCl_2COO)_3{\cdot}H_2O$ [12] with Y(4-bpy)$_2(CCl_3COO)_3{\cdot}H_2O$ **I** and Y(4-bpy)$_{1.5}(CHBr_2COO)_3{\cdot}3H_2O$ **III**, we notice that their thermal stability in air is very similar: (328–333 K). It changes for anhydrous species: Y(4-bpy)$(CHCl_2COO)_3$ [12] (403 K) >Y(4-bpy)$_{1.5}(CHBr_2COO)_3$ **III** (373 K) >Y(4-bpy)$_2(CCl_3COO)_3$ **I** (353 K).

In the case of lanthanum(III) complexes, the thermal stability in air presents in the following line:

La(4-bpy)$(CHBr_2COO)_3{\cdot}H_2O$ **IV** (373 K) = La(4-bpy)$(CHCl_2COO)_3{\cdot}H_2O$ [6] (373 K) > La(4-bpy)$_{1.5}(CCl_3COO)_3{\cdot}2H_2O$ **II** (333 K).

and after dehydration:

La(4-bpy)$(CHCl_2COO)_3$ [6] (433 K) > La(4-bpy)$(CHBr_2COO)_3$ **IV** (418 K) > La(4-bpy)$_{1.5}(CCl_3COO)_3$ **II** (413 K).

The TG-FTIR study also suggests several steps of thermolysis in argon atmosphere. The first process is dehydration containing elevation of water. When temperature rises, partial and total decomposition of organic ligands takes place. The gas evolved contains mainly H_2O, CO_2, CO, hydrocarbons, and mixture of volatile organic fragments coming from decomposition of appropriate halogenoacetates.

In summary, the investigation in this paper complete the information of the solid species containing 4,4′-bipyridine and dichloro- or trichloroacetates in the lanthanide series:

Y, La → Lu without Pm (obtained in similar manner), additionally some information about Ln(III) species with 4,4'-bipyridine and monochloroacetates [13].

Acknowledgements We thank students M. Niedźwiecki and D. Więzowski for participation in experimental part of this work.

References

1. Łyszczek R. Synthesis, structure, thermal and luminescent behavior of lanthanide: pyridine-3,5-dicarboxylate frameworks series. Thermochim Acta. 2010;509:120–7. doi:10.1016/j.tca.2010.06.010.
2. Batten A, Robson R. Interpenetrating nets: ordered, periodic entanglement. Angew Chem Int Ed. 1998;37:1461–94. doi:10.1002/(SICI)1521-3773(19980619).
3. Janiak C. Functional organic analogues of zeolites based on metal–organic coordination frameworks. Angew Chem Int Ed Engl. 1997;36:1431–4. doi:10.1002/anie.199714311.
4. Tao J, Tong ML, Chen XM. Hydrothermal synthesis and crystal structures of three-dimensional co-ordination frameworks constructed with mixed terephthalate (tp) and 4,4′-bipyridine (4,4′-bipy) ligands: [M(tp)(4,4′-bipy)] (M = Co^{II}, Cd^{II} or Zn^{II}). J Chem Soc Dalton Trans. 2000;3669–74.
5. Zaworotko MJ. Superstructural diversity in two dimensions: crystal engineering of laminated solids. Chem Commun. 2001;1:1–9.
6. Czylkowska A, Kruszyński R, Czakis-Sulikowska D, Markiewicz M. Coordination polymer of lanthanum: synthesis, properties and crystal structure of $[La(4,4'\text{-bipyridine})(CCl_2HCOO)_3(H_2O)]_n$. J Coord Chem. 2007;60:2659–69. doi:10.1080/00958970701299550.
7. Rohde A, Urland W. Catena-Poly[[(2,2′-bipyridine-j2N,N′)-neodymium(III)]-l-dichloroacetato-1j2O:O′:2jOdi-l-dichloroacetato-j4O:O]. Acta Crystallogr Sec E. 2006;62(7):m1618–9. doi:10.1107/S1600536806022872.
8. Rohde A, Urland W. Catena-Poly[[(2,2′-bipyridine-j2N,N′)-praseodymium(III)]-l-dichloroacetate-1j2O:O′:2jO-di-l-dichloroacetato-j4O:O′]. Acta Crystallogr Sec E. 2006;62(11):m2843–5. doi:10.1107/S160053680603995X.
9. John D, Urland W. Synthesis, crystal structure, and magnetic behaviour of $[Gd_2(ClF_2CCOO)_6(H_2O)_2(bipy)_2]_2{\cdot}C_2H_5OH$. Z Anorg Allg Chem. 2006;632(10):1768–70. doi:10.1002/zaac.200500400.
10. John D, Urland W. Crystal structure and magnetic behaviour of the new gadolinium complex compound $Gd_2(ClH_2CCOO)_6(bipy)_2$. Eur J Inorg Chem. 2005;22:4486–9. doi:10.1002/ejic.200500734.
11. Rohde A, John D, Urland W. Crystal structures of $Gd_2(Cl_3CCOO)_6(bipy)_2(H_2O)_2{\cdot}$4-bipy, $Pr(Cl_3CCOO)_3(bipy)_2$, $Nd(Cl_3CCOO)_3(bipy)_2$ and $Er(Cl_3CCOO)_3(bipy)_2(H_2O)$. Z. Kristal. 2005;220(2):177–82. doi:10.1524/zkri.220.2.177.59141.
12. Czakis-Sulikowska D, Czylkowska A, Markiewicz M. Synthesis, characterization and thermal decomposition of yttrium and light lanthanides with 4,4′-bipyridine and dichloroacetates. Polish J Chem. 2007;81:1267–75.
13. Czylkowska A. New complexes of heavy lanthanides with 4,4′-bipyridine and trichloroacetates; Synthesis, thermal and other properties. J Therm Anal Calorim (in press). doi:10.1007/s10973-011-2041-4 references therein and unpublished data.
14. Powder Diffraction File, PDF-2, release 2004. The International Centre for Diffraction Data (ICDD). 12 Campus Boulevard, Newton Square, PA, USA.
15. Geary WI. The use of conductivity measurements in organic solvents for the characterisation of coordination compounds. Coord Chem Rev. 1971;7:81–122. doi:10.1016/S0010-8545(00)80009-0.
16. Pearce CK, Grosse DW, Hessel W. Effect of molecular structure on infrared spectra of six isomers of bipyridine. Chem Eng Data. 1970;15:567–70. doi:10.1021/je60047a042.
17. Zelenak V, Vargova Z, Gyoryova K. Correlation of infrared spectra of zinc(II) carboxylates with their structures. Spectrochimica Acta A. 2007;66:262–72. doi:10.1016/j.saa.2006.02.050.
18. Brzyska W, Dębska E, Szczotka M. New complexes of rare earth elements with methylsuccinic acid. Polish J Chem. 2001;75:1393–9.
19. Deacon GB, Philips RI. Relationships between the carbon-oxygen stretching frequencies of carboxylato complexes and the type of carboxylate coordination. Coord Chem Rev. 1980;33:227–50. doi:10.1016/S0010-8545(00)80455-5.
20. Nakamoto K. Infrared and Raman spectra of inorganic and coordination compounds. New York: Wiley and Sons; 2009.
21. Manhas BS, Trikha AK. Relationships between the direction of shifts in the carbon-oxygen stretching frequencies of carboxylato complexes and the type of carboxylate coordination. Indian J Chem. 1982;59:315–9.
22. Brzyska W, Ożga W. Spectral, magnetic and thermal investigations of some *d*-electron element 3-methoxy-4-methylbenzoates. J Therm Anal Calorim. 2006;84:385–9. doi:10.1007/s10973-005-6855-9.
23. Zapata B, Balmaseda J, Fregoso-Israel E, Torres-Garcia E. Thermo-kinetics study of orange peel in air. J Therm Anal Calorim. 2009;98:309–15.